

# Voltammetric and morphological characterization of zinc electrodeposition from acid electrolytes containing boric–polyalcohol complexes

E. M. de Oliveira · I. A. Carlos

Received: 24 October 2007 / Revised: 26 February 2008 / Accepted: 26 February 2008 / Published online: 13 March 2008  
© Springer Science+Business Media B.V. 2008

**Abstract** The influence of sorbitol or glycerol polyalcohols on the electrodeposition of zinc and on morphology of the zinc film is discussed. The deposition current efficiency, in the potential range  $-1.30$  V to  $-2.50$  V, was  $\sim 90\%$  in all baths. Increasing the sorbitol concentration in the bath shifted the deposition to more negative potentials,  $\sim 50$  mV, and decreased the current density ( $j_p$ ) of the zinc deposition significantly. On the other hand, adding glycerol did not significantly affect either  $j$  or the deposition potential of zinc. Scanning electron microscopy (SEM) showed that either sorbitol or glycerol lead to the formation of granular deposits. The best zinc morphology was obtained with  $0.52$  M sorbitol or glycerol in the plating bath. The presence of sorbitol or glycerol in the plating bath was beneficial, since the resulting zinc deposits were compact and without holes.

**Keywords** Electrodeposition · Zinc · Sorbitol–boric complex · Glycerol–boric complex

## 1 Introduction

Zinc electrocoatings have for a long time been widely used to protect steel from corrosion and there is a considerable record of data on zinc electrodeposition in different electrolytic solutions [1]. Organic and inorganic compounds in the electrolyte play an important role in metal plating, as they facilitate the formation of uniform overlayers of high brightness. Such additives do not take part in the deposition

reaction directly but they influence the nucleation and growth of the deposit and consequently the film morphology [2].

Lee et al. [3] studied the effects of organic additives such as benzoic acid (BA) and polyethylene glycol (PEG) on the initial stages of zinc electroplating. BA mainly contributed to the control of roughness of the zinc layer, interacting weakly with zinc ions. However, PEG molecules raise the overpotentials for reduction of both zinc ions and protons by effectively blocking the electrode surface. Mackinnon and Brannen [4] studied the effects of adding various organic compounds to a  $ZnCl_2$  electrolyte on zinc deposit morphology and crystallite orientation. Tetrabutylammonium chloride (TBACl) was the most effective of several tetraalkylammonium chlorides in smoothing and refining the grain and eliminating dendritic growth. Robinson and O'Keefe [5] studied the effects of antimony and glue on zinc electrowinning and concluded that antimony refined the grain size and glue leveled the deposits by preventing dendritic growth. Mackinnon et al. [6] studied the effect of thiourea, with and without the addition of glue and antimony, on the zinc deposition current efficiency (CE), as well as on the morphology and orientation of zinc deposits. Increasing concentrations of thiourea decreased the CE and the additional presence of antimony did not significantly alter this effect, which the addition of glue resulted in a further substantial decrease in CE. Thiourea changed the zinc deposit morphology and orientation, and altered the shape of the zinc deposition cyclic voltammogram. Zinc electrodeposition at high current density was studied by Karavasteva and Karaivanov [7] and Thomas and Fray [8]. The first authors investigated the effect of some surfactants on the structure of the deposit, current density, cell voltage, specific energy consumption and the purity of zinc metal electroextracted at

E. M. de Oliveira · I. A. Carlos (✉)  
Departamento de Química, Universidade Federal de São Carlos,  
CP 676, Sao Carlos, SP 13565-905, Brazil  
e-mail: diac@ufscar.br

high current density under simulated industrial conditions. They found that at high current density, a pore-free and fine-grained zinc deposit can be obtained only in the presence of suitable additives. Thomas and Fray [8] also showed that zinc can be deposited electrochemically at high current densities ( $200 \text{ mA cm}^{-2}$ ), and that protein additives produced planar deposits with (102) and (103) crystal orientations and a current efficiency of around 85%. Chandran [9] showed that the addition of vanillin as a brightener to the plating bath led to bright deposits, which afforded good corrosion resistance.

It has been observed in our laboratory that electrodeposition of pure metals or alloys from a plating bath containing the polyalcohol sorbitol or glycerol leads to metal or alloy films with smooth surface and that even in the potential region of vigorous hydrogen evolution, the films do not burn, suggesting that these polyalcohols prevent the deposits from becoming darker [10–16].

Hence, motivated by these results, we decided to investigate the influence of sorbitol or glycerol in the electrolyte on the zinc deposition process and on the zinc film morphology. The effects of these polyalcohol additives were studied by voltammetry and scanning electron microscopy (SEM).

## 2 Experimental details

All experiments were carried out at room temperature ( $25^\circ\text{C}$ ), in a glass single-compartment cell of 50 mL capacity. A platinum disc ( $0.16 \text{ cm}^2$ ), a platinum plate and a calomel electrode (1 M KCl) were employed as working, auxiliary and reference electrodes, respectively. Immediately before each experiment, the Pt working electrode was ground with  $0.3 \mu\text{m}$  alumina, immersed in concentrated sulphuric–nitric acid solution and then rinsed with deionized water. The zinc electrodeposits were obtained from the baths described in Table 1. The initial pH of some plating baths (Zn1; Zn1 + 0.26 M glycerol; Zn1 + 0.39 M glycerol and Zn2 + 0.52 M glycerol) were  $\sim 4.00$ . However, after several voltammetric deposition cycles it was found that the pH had changed to  $\sim 3.00$ . Thus, the pH of these

solutions (without and with glycerol ( $\text{C}_3\text{H}_8\text{O}_3$ )) was accurately adjusted at 3.00 with  $\text{H}_2\text{SO}_4$ . For electrolytic solutions containing sorbitol ( $\text{C}_6\text{H}_{14}\text{O}_6$ ), the initial pH was 2.80 (0.26 M sorbitol), 2.60 (0.39 M sorbitol) and 2.50 (0.52 M sorbitol) and was maintained constant after several voltammetric deposition cycles. The deposition current efficiency (CE) was calculated from the stripping/deposition charge ratio. The Zn films were obtained with a deposition time of 40 s. The Zn deposit stripping solution was 1 M  $\text{NH}_4\text{Cl}$  adjusted to  $\text{pH} = 2.00$  with HCl. Potentiodynamic studies were carried out using a scanning potentiostat (PAR model 173). pH measurements were made with a Micronal B474 pH meter. Scanning electron microscopy (SEM) measurements were made with a ZEISS DSM 960 (West Germany).

## 3 Results and discussion

### 3.1 Potentiodynamic study

Figure 1a and b shows the cathodic and anodic voltammetric curves from Zn1 solution (0.55 M  $\text{ZnSO}_4$  + 0.13 M  $\text{H}_3\text{BO}_3$ ). It can be seen that a cathodic wave *c* occurs (Fig. 1a, dashed and solid lines, and Fig. 1b, solid line) before bulk zinc deposition ( $-1.18 \text{ V}$ , Fig. 1a, solid line). In the return sweep, there are two anodic peaks  $a_1$  (Fig. 1a, dashed and solid lines, and Fig. 1b, solid line) and  $a_2$  (Fig. 1a, solid line). The peak  $a_2$ , associated with zinc dissolution, is formed only when the sweep is reversed at potentials more negative than  $-1.18 \text{ V}$  (Fig. 1a, solid line). Also, the anodic peak  $a_1$  is directly related to cathodic wave *c*, as can be seen in Fig. 1a and b. Moreover, it was found that for potentials less negative than  $-0.20 \text{ V}$  (Fig. 1b, dashed line) the reduction process had a charge density of  $3 \text{ mC cm}^{-2}$ . However, in the anodic sweep the peak  $a_1$  cannot be seen (Fig. 1b, dashed line), due probably to the small amount of the species formed during the cathodic scan from  $+0.5 \text{ V}$  to  $-0.2 \text{ V}$ .

The cathodic wave *c* might be related to zinc deposition at an under potential (UPD) or adsorption of a species present in the plating bath. However, it cannot be related to zinc UPD, since the charge density of this wave is  $24.1 \text{ mC cm}^{-2}$ , far from the zinc monolayer charge density of  $\sim 460 \mu\text{C cm}^{-2}$  [17]. Although, borate anion adsorption has been reported to occur during the cathodic process [17–19], in the present study borate anion adsorption can be disregarded, since at this acid pH (3.00) dissociation of boric acid is negligible [20] and, consequently, uncharged boric acid predominates over borate in the zinc plating bath. Other possibilities are that wave *c* could be related to atomic hydrogen adsorption (AHA) and/or hydrogen evolution reaction (HER) and the anodic peak  $a_1$  to desorption

**Table 1** Composition of zinc plating baths

Baths	Baths
Zn1*	
Zn1 + 0.26 M Sorbitol	Zn1 + 0.26 M Glycerol
Zn1 + 0.39 M Sorbitol	Zn1 + 0.39 M Glycerol
Zn2** + 0.52 M Sorbitol	Zn2 + 0.52 M Glycerol

Zn1\* = 0.55 M  $\text{ZnSO}_4$  + 0.13 M  $\text{H}_3\text{BO}_3$

Zn2\*\* = 0.55 M  $\text{ZnSO}_4$  + 0.26 M  $\text{H}_3\text{BO}_3$

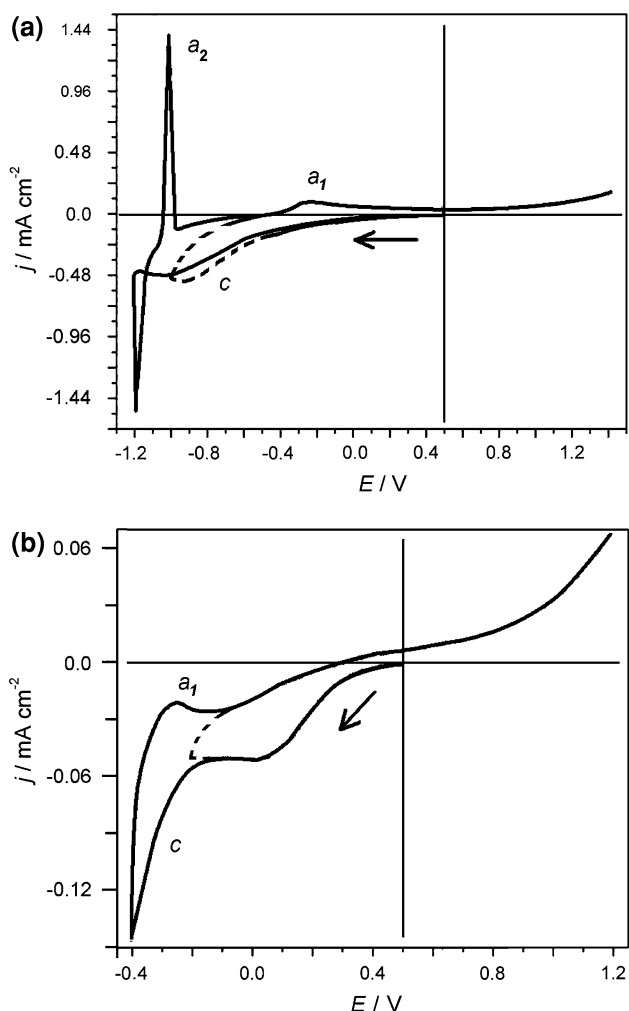


**Fig. 1** Voltammetric curves for Pt substrate in solution Zn1 (Table 1); effect of varying the cathodic potential limit ( $E_p$ ): (a)  $-1.00$  V (- -) and  $\sim -1.19$  V (—); (b)  $-0.2$  V (- -) and  $-0.40$  V (—).  $v = 10$   $\text{mV s}^{-1}$

of atomic hydrogen and/or molecular hydrogen oxidation. It must be pointed out that during the formation of wave *c*,  $\text{H}_2$  bubbles were visible to the naked eye on the platinum electrode.

Wopschall and Shain report [21] that the adsorption peak current increases approximately linearly with scan rate while the diffusion peak current increases approximately as the square root of scan rate [21, 22]. Figure 2b shows the peak current density ( $j_p$ ) plotted against the square root of sweep rate ( $v^{1/2}$ ). The  $j_p$  were obtained of the voltammetric curves for the Pt electrode in electrolytic solution Zn1 at several sweep rates (Fig. 2a). It can be seen in Fig. 2b that  $j_p$  increased linearly with increasing  $v^{1/2}$ . Thus, the process occurring in the region of wave *c*, is controlled by mass transport. Moreover, it is reported in the literature that atomic hydrogen adsorption or desorption charge density on a Pt electrode is not influenced by sweep rate [23, 24], implying that wave *c* is related to the HER.

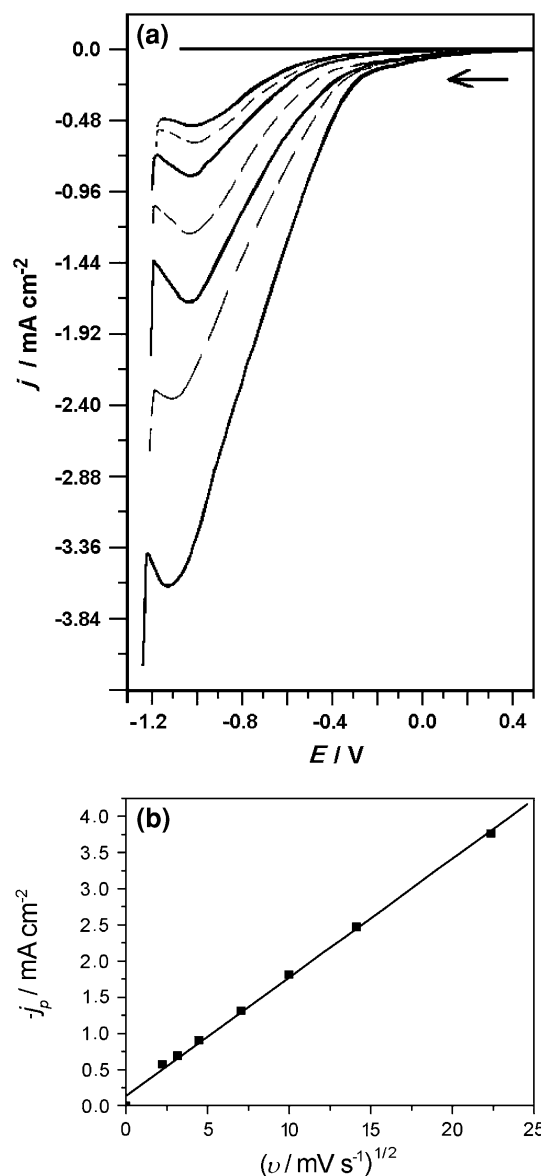


**Fig. 2** (a) Voltammetric curves for a platinum substrate in Zn1 at various sweep rates ( $v/\text{mV s}^{-1}$ ): (a) 5 (—); 10 (—); 20 (—); 50 (—); 100 (—); 200 (—); 500 (—); (b) Graphs of peak current density vs. square root of sweep rate

Thus, to test this hypothesis, variation of  $q_c$  as a function of the pH of the Zn1 plating bath (pH: 4.00 and 2.25) and the influence of rotation frequency ( $f$ ) of a rotating disk electrode (RDE) on the current density of wave *c* were recorded (Fig. 3). It can be seen that the charge density of wave *c* increases when the pH of the solution falls from 4.00 (—) to 2.25 (— · —), with  $f = 0$  Hz. This result confirms that the process occurring in the region of wave *c* is related to the HER, because the higher the  $\text{H}^+$  ion concentration in the plating bath, the more significant is this reaction [25]. In addition, the current density of wave *c* increased as the rotation frequency ( $f$ ) rose from 0 Hz (— · —) to 5 Hz (— • —) and 10 Hz (— • • —), indicating that the process

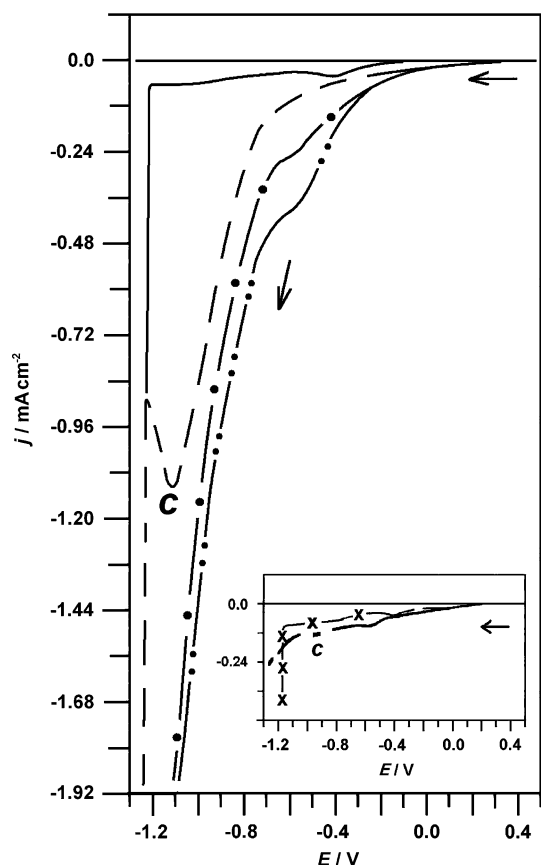


**Fig. 3** Cathodic voltammetric curves for Pt substrate in electrolytic solution: Zn1 pH 4.00 (—); Zn1 pH 2.25 (---); Zn1 pH 2.25 with RDE,  $f = 5$  Hz (—•—) and Zn1 pH 2.25 with RDE,  $f = 10$  Hz (—••—); Inset: 0.55 M  $\text{ZnSO}_4$  (—x—) and 0.13 M  $\text{H}_3\text{BO}_3$  (---).  $v = 10 \text{ mV s}^{-1}$

occurring in the region of wave *c* is controlled by mass transfer. These results corroborate those shown in Fig. 2b. The inset in Fig. 3 shows voltammetric curves for a platinum substrate in two different solutions: 0.55 M  $\text{ZnSO}_4$  (—x—) and 0.13 M  $\text{H}_3\text{BO}_3$  (---). The pH of these solutions was adjusted precisely to 4.00 with  $\text{H}_2\text{SO}_4$ . It can be seen that the current densities of wave *c* are similar in both solutions and also similar to Zn1 (—), Fig. 3. Hence, the presence of zinc ions in the electrolytic solution did not affect the process occurring in the region of wave *c*, which therefore cannot be related to zinc deposition, corroborating the results above.

In sum wave *c* is related to the HER and the anodic peak  $a_1$  to oxidation of molecular hydrogen produced by the HER.

### 3.2 Study of deposition process in the presence of polyalcohols

An electrochemical study of zinc deposition was carried out in baths containing sorbitol or glycerol to discover whether these additives influenced this process.

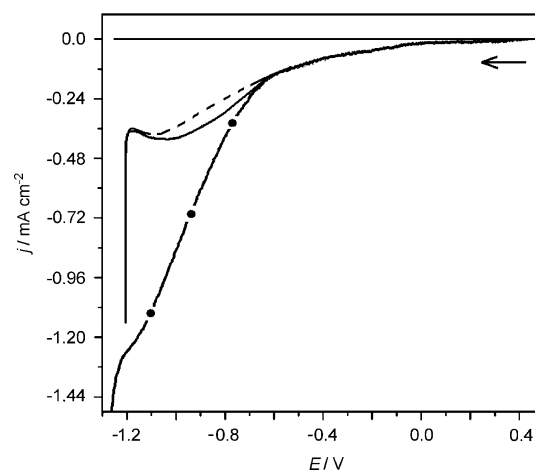


**Fig. 4** Zn deposition voltammetric curves from Zn1, pH 3.00 (—); Zn2 + 0.52 M glycerol, pH 3.00 (---) and Zn2 + 0.52 M sorbitol, pH 2.50 (—•—) electrolytic solutions

Figure 4 shows the voltammetric curves of the cathodic process occurring in the region of wave *c* (initial moments of the reduction process), in the absence and presence of glycerol or sorbitol. It can be seen that there is an increase in the current density in the region of wave *c* (HER) in Zn2 + 0.52 M sorbitol, which can be attributed to the presence of sorbitol. Voltammetric curves for Pt electrode from electrolytic solution 0.55 M  $\text{NaSO}_4$  + 0.26 M  $\text{H}_3\text{BO}_3$  containing 0.52 M glycerol or 0.52 M sorbitol at pH 3.00 for all baths were carried out (Figures not shown). It was verified in these Figures that the current density in the initial moments of cathodic process, in the presence of sorbitol, was higher than in the absence or presence of glycerol. Thus, it can be inferred from that sorbitol catalyze the HER on to Pt in the initial moments of cathodic process.

Figure 5a and b shows voltammetric curves of zinc deposition from plating baths containing various sorbitol or glycerol concentrations, respectively. It can be observed in Fig. 5a that an increase in sorbitol concentration leads to a shift in the deposition potential to more negative potentials; thus, a shift of  $\sim 50$  mV occurred at 0.52 M sorbitol in the plating bath. It is reported in the literature that boric acid inhibits zinc deposition [17]. In our previous work, this inhibition is attributed to adsorption of boric acid–polyalcohol complexes on the platinum surface [10]. Furthermore, it may be noted in Fig. 5a that the deposition current density ( $j$ ) decreased significantly with increasing additive concentration. With 0.52 M of sorbitol in the plating bath, peak deposition current density ( $j_p$ ) decreased 25%. In contrast, Fig. 5b shows that the glycerol at the same molarities did not significantly alter  $j$  or the deposition potential of zinc from the values in the absence of this additive (—).

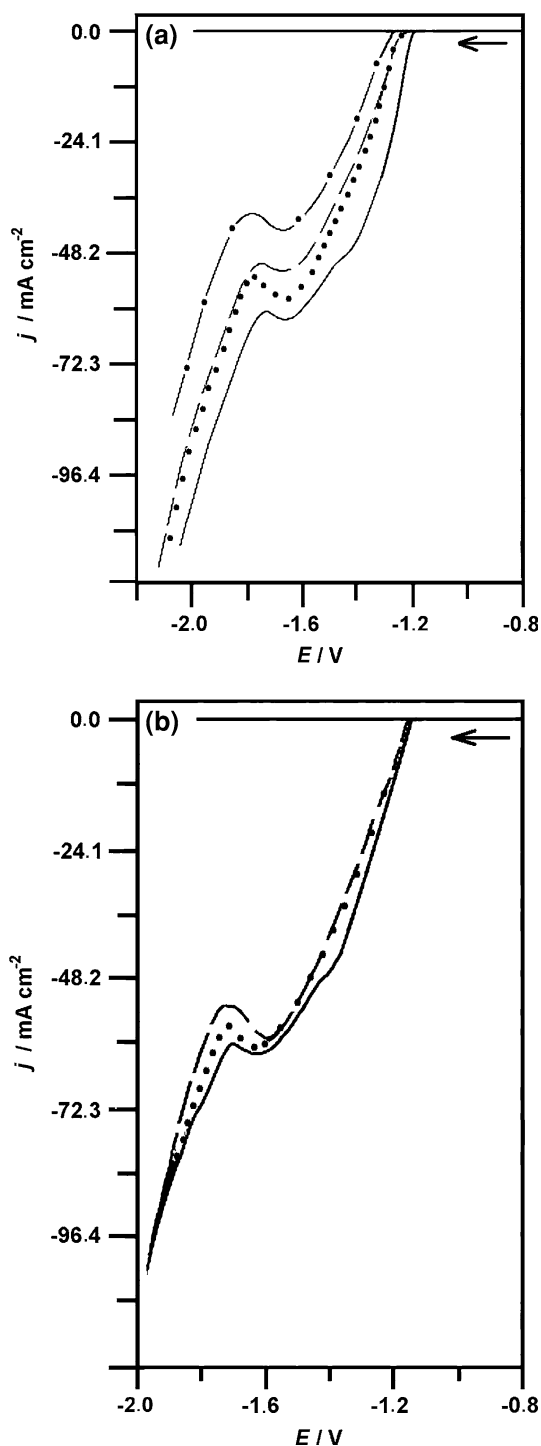


**Fig. 5** Zn deposition voltammetric curves from electrolytic solutions: (a) Zn1 (—); Zn1 + 0.26 M sorbitol (•••); Zn1 + 0.39 M sorbitol (- -) and Zn2 + 0.52 M sorbitol (- • -); (b) Zn1 (—); Zn1 + 0.26 M glycerol or Zn1 + 0.39 M glycerol (•••) and Zn2 + 0.52 M glycerol (- -).  $v = 10 \text{ mV s}^{-1}$

Comparing Fig. 5a and b it can be seen that the current densities in the sorbitol baths are lower than those in the corresponding glycerol baths. This is probably due to the size of the adsorbed boric–sorbitol complex ( $\text{H}_3\text{BO}_3 \cdot 2\text{C}_6\text{H}_{14}\text{O}_6$ ), which is much larger than the boric–glycerol complex ( $\text{H}_3\text{BO}_3 \cdot 2\text{C}_3\text{H}_8\text{O}_3$ ) and consequently blocks more effectively the deposition process [10]. Moreover, it was obvious when handling the electrolytes that the solutions containing sorbitol were more viscous than those with glycerol.

Further insight into the zinc deposition process from solutions containing polyalcohol was gained when the cathodic sweep was reversed at various final potentials ( $E_f$ ) in baths with and without additive. Figure 6 shows typical voltammetric curves recorded from Zn1 and Zn2 + 0.52 M sorbitol solutions at  $E_f = -1.85 \text{ V}$ . It can be seen that on reversal of the sweep, the cathodic current density in the absence of sorbitol increased (—), while in its presence (—•—) it decreased. The increase in the current density on reversal (—) can probably be attributed to an increase in the area of zinc electrodeposit obtained in the absence of additive (as will be seen better in Sect. 3.3).

The anodic process (Fig. 6, dashed and solid line) shows an anodic peak of zinc dissolution in the presence and absence of the boric–sorbitol complex in the plating bath. It can be inferred from these curves that this complex hinders zinc dissolution, since the anodic peak potential was shifted  $\sim 50 \text{ mV}$  in the positive direction in the presence of boric–sorbitol complex. This result corroborates those obtained by Pereira et al. [26] who report that Zn electrode

shows an anodic peak of zinc dissolution in the presence and absence of the boric–sorbitol complex in the plating bath. It can be inferred from these curves that this complex hinders zinc dissolution, since the anodic peak potential was shifted  $\sim 50 \text{ mV}$  in the positive direction in the presence of boric–sorbitol complex. This result corroborates those obtained by Pereira et al. [26] who report that Zn electrode

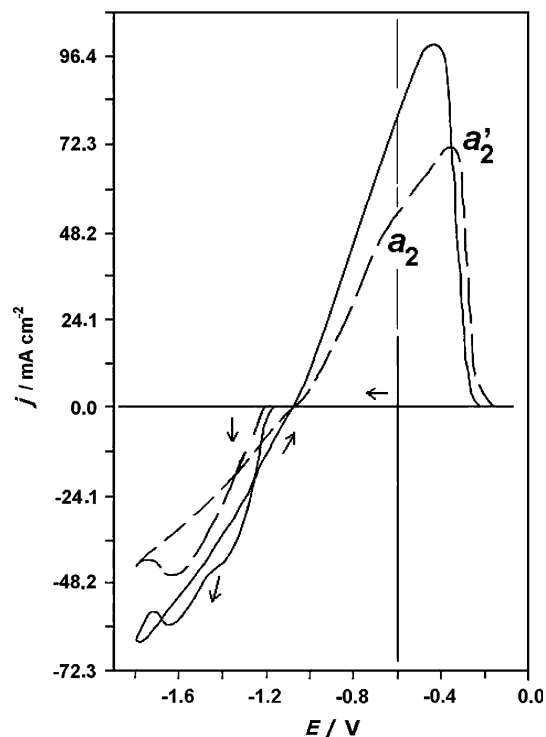


**Fig. 6** Zn deposition and dissolution voltammetric curves from electrolytic solutions: Zn1 (—) and Zn2 + 0.52 M sorbitol (- -), cathodic limit potential ( $E_f$ ):  $-1.85 \text{ V}$ .  $v = 10 \text{ mV s}^{-1}$

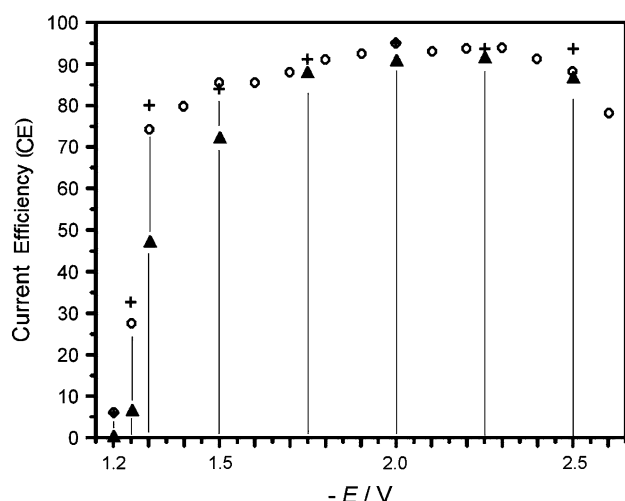


**Fig. 7** Zinc deposition current efficiency (CE) at several deposition potentials and a deposition time of 40 s. Plating baths: Zn1 (○), Zn2 + 0.52 M sorbitol (▲) and Zn2 + 0.52 M glycerol (+)

dissolution is inhibited in an alkaline electrolyte containing sorbitol concentrations higher than 0.20 M.

Similar results were obtained at different  $E_f$  ( $-1.35$  V and  $-1.55$  V). Also, it was noted that the voltammetric dissolution of zinc film produced in a plating bath containing glycerol was similar to that in the absence of additive (Fig. 6 (—)).

Figure 7 demonstrates the effect of varying the deposition potential on the current efficiency (CE) of the zinc electrodeposition process. The zinc films were obtained chronoamperometrically from  $+0.50$  V at various deposition potentials ( $E_d$ ). The CE values obtained at different  $E_d$  are within an error of 5%. It can be seen in Fig. 7 that CE values increase as the deposition potential becomes more negative, irrespective of the composition of the bath used. Also, the CE values were lower than 100%, due to the HER taking place simultaneously. The low CE values obtained at  $-1.20$  V and  $-1.25$  V are due to the slow zinc deposition rate at these potentials, which correspond to the initial moments of the voltammetric deposition process. Thus, in these cases the contribution of the HER to the deposition process, is more significant than at more negative potentials.

It must be stressed that at potentials more negative than  $-2.50$  V, it was not possible to calculate the CE values, due to the formation of dendritic Zn deposits that peel off the platinum substrate.

### 3.3 Scanning electronic microscopy

Scanning electron microscopy (SEM) was used to establish the relationship between the sorbitol or glycerol concentration in the plating bath and zinc film morphology.

Figure 8a–g shows SEM micrographs of zinc films obtained from Zn1 in the absence and presence of various sorbitol or glycerol concentrations (Table 1) at  $-1.85$  V and a charge density of  $4.0$  C cm $^{-2}$ . The zinc films obtained in the presence of both additives had a granular structure. Although significant differences in the morphology of the zinc film were not seen in the presence of various sorbitol concentrations (average size of zinc crystallites was  $\sim 2$   $\mu$ m), the grain structure of the zinc film obtained in the presence of 0.52 M sorbitol (Fig. 8d) was more compact than at other sorbitol concentrations. However, for zinc deposits obtained from baths containing glycerol, there was a decrease in the grain size from  $\sim 3$   $\mu$ m (Fig. 8e, f) to  $\sim 1$   $\mu$ m (Fig. 8g), when the glycerol concentration increased to 0.52 M in the plating bath.

Comparing the grain size of deposits obtained from baths containing 0.26 M sorbitol (Fig. 8b) or 0.39 M sorbitol (Fig. 8c) with those from the same glycerol molar concentrations (Fig. 8e, f), it can be seen that the grains in the former deposits were smaller (2  $\mu$ m) than those in the latter (3  $\mu$ m). For both additives in the deposition bath, the best zinc morphology was obtained at 0.52 M. Also, the zinc films obtained in the presence of 0.52 M glycerol (Fig. 8g), showed crystallites more refined than with sorbitol in the plating bath (Fig. 8d). Moreover, the zinc crystallites obtained in the presence of sorbitol showed hexagonal characteristics, while the ones in the presence of glycerol showed various forms.

Finally, it was confirmed that the zinc film obtained in the absence of polyalcohol showed holes in its morphological structure (Fig. 8a). It can be concluded that the presence of polyalcohol in the plating bath was beneficial, since the zinc deposits were more compact.

### 3.4 Influence of the pH in Zn2 + 0.52 M sorbitol plating bath

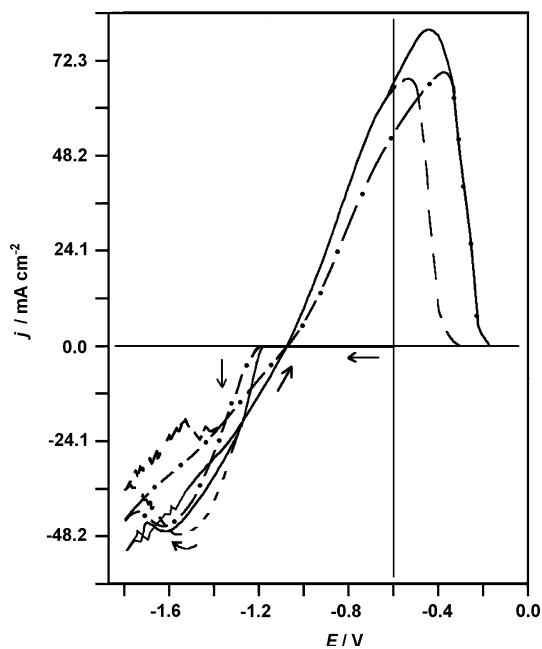
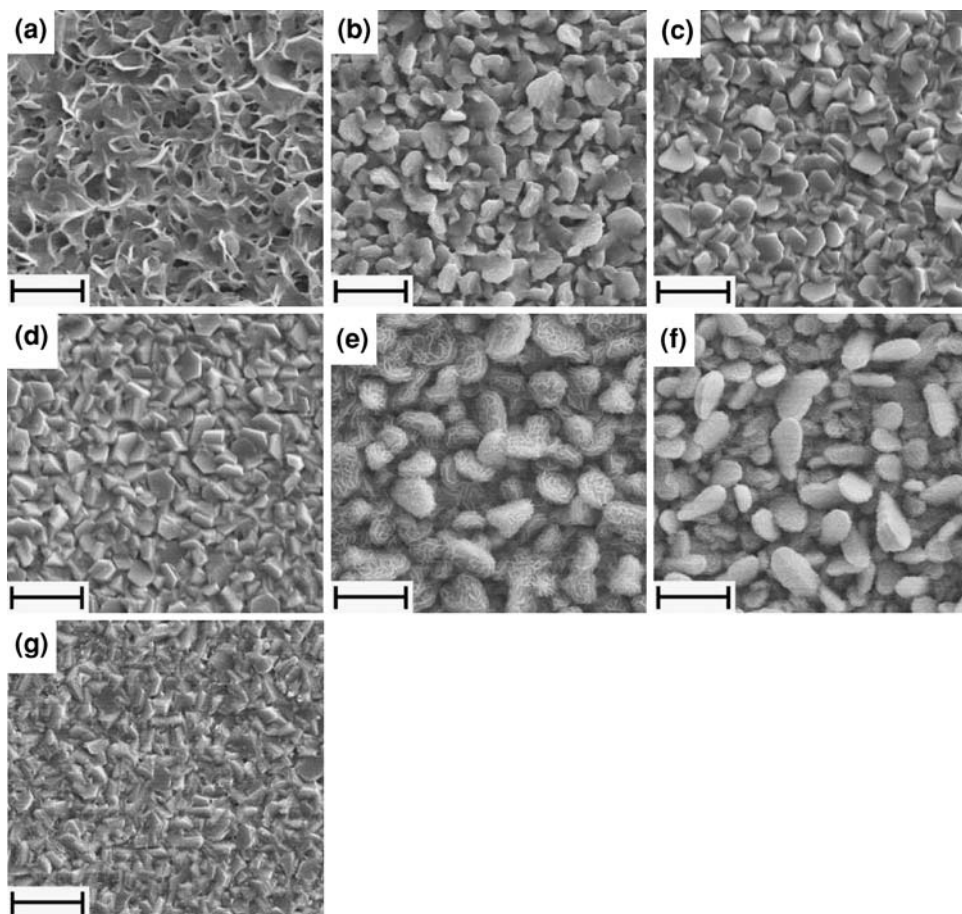
The effect of varying the bath pH was studied. The pH of the unadjusted plating bath Zn2 + 0.52 M sorbitol (pH = 2.50) remains unchanged even after extensive use of this solution for zinc voltammetric deposition. Thus, this bath was chosen for further studies.

Figure 9 illustrates the zinc deposition and dissolution from Zn2 + 0.52 M sorbitol at various pHs: 2.50 (—●—), pH 3.95 (—) and pH 5.60 (—•—). The pH of the bath was adjusted accurately to 3.95 or 5.60 with NaOH. Varying the pH had practically no effect on either the potentials or the currents of the plating process.

SEM micrographs of zinc films obtained with Zn2 + 0.52 M sorbitol at various pH (pH = 2.50, Fig. 8d; pH = 3.95, Fig. 10a and pH = 5.60, Fig. 10b) showed that increasing the pH produced an increase in roughness and the zinc film obtained from Zn2 + 0.52 M sorbitol at



**Fig. 8** SEM micrographs of Zn films obtained chronoamperometrically from  $-0.60$  V to  $-1.85$  V with  $4.0 \text{ C cm}^{-2}$ . Electrolytic solutions: (a) Zn1; (b) Zn1 + 0.26 M sorbitol; (c) Zn1 + 0.39 M sorbitol; (d) Zn2 + 0.52 M sorbitol; (e) Zn1 + 0.26 M glycerol; (f) Zn1 + 0.39 M glycerol and (g) Zn2 + 0.52 M glycerol;  $4 \mu\text{m}$  |—|



**Fig. 9** Zn deposition and dissolution voltammetric curves obtained from electrolytic solution Zn2 + 0.52 M sorbitol at various pH: 2.50 (—•—); 3.95 (—) and 5.60 (—).  $v = 10 \text{ mV s}^{-1}$

pH 5.60 (Fig. 10b), showed the formation of some dendritic crystallites. It is reported in the literature that the HER in parallel with metal deposition acts as a leveller [27]. It can thus be inferred that the Zn film obtained from the bath at pH = 2.50 (Fig. 8d) was probably less rough due to HER in parallel with Zn deposition.

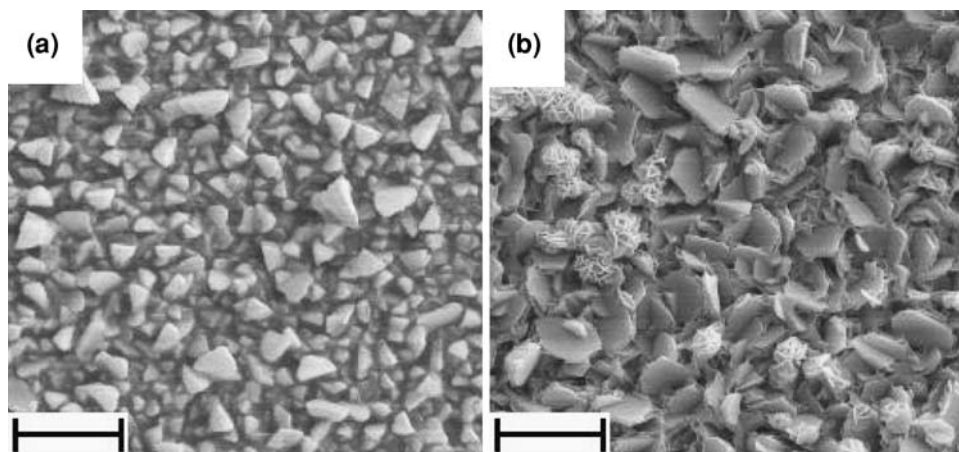
It can be concluded that lowering the bath pH results in a more compact and smooth zinc film.

#### 4 Conclusions

We have carried out electrodeposition of zinc using  $0.55 \text{ M ZnSO}_4 + 0.13 \text{ M H}_3\text{BO}_3$  as the electrolytic solution, with and without the addition of various concentrations of sorbitol or glycerol.

Potentiodynamic measurements and SEM micrographs were used to determine the influence of the polyalcohol additives sorbitol or glycerol, on the deposition process and zinc film morphology, respectively. The HER started before bulk zinc deposition occurred in the cathodic sweep and its rate was found to depend on the solution pH and rotation frequency of the Pt substrate.

**Fig. 10** SEM micrographs of Zn films obtained chronoamperometrically from  $-0.60$  V to  $-1.85$  V with  $4.0 \text{ C cm}^{-2}$ . Electrolytic solution  $\text{Zn}^{2+} + 0.52 \text{ M}$  sorbitol at two different pH: (a) 3.95 and (b) pH 5.60.  $4 \mu\text{m}$   $\text{—|—}$



As the sorbitol content rose, there was a shift in the deposition potential to more negative values. Thus, at  $0.52 \text{ M}$  sorbitol, the initial deposition potential was about  $50 \text{ mV}$  more negative than without sorbitol. Also, the current density of zinc deposition decreased significantly as sorbitol was added; at  $0.52 \text{ M}$  of sorbitol in the plating bath,  $j_p$  decreased  $25\%$ . On the other hand, the glycerol additive did not significantly affect  $j$  or deposition potential of zinc.

The deposition current efficiency (CE) in the potential range of  $-1.30 \text{ V}$  to  $-2.50 \text{ V}$  was  $\sim 90\%$ , for all baths. The zinc morphology in the presence of sorbitol or glycerol polyalcohols showed a granular structure. The average size of zinc crystallites in the films obtained in the presence of any sorbitol concentration was  $\sim 2 \mu\text{m}$ . In baths containing glycerol, the size decreases from  $\sim 3 \mu\text{m}$  to  $\sim 1 \mu\text{m}$  at the highest concentration of this additive in the plating bath.

With  $0.52 \text{ M}$  sorbitol or glycerol in the plating bath, the best zinc morphology was obtained, with smaller crystallites and more compact film. The zinc crystallites were more refined in the films obtained in the presence of  $0.52 \text{ M}$  glycerol. The zinc bath containing  $0.52 \text{ M}$  sorbitol (pH = 2.50) resulted in a more compact and smoother film than did the baths at pH = 3.95 or pH = 5.60.

The presence of polyalcohol in the plating bath was beneficial, since zinc deposits were compact and hole-free.

**Acknowledgements** Financial support from the Brazilian agencies CNPq (Proc. 303670/2007-0) is gratefully acknowledged.

## References

1. Barcelo G, Sarret M, Muller C, Pregonas J (1998) *Electrochim Acta* 43:13
2. Cruz MS, Alonso F, Palacios JM (1993) *J Appl Electrochem* 23:364
3. Lee JY, Kim JW, Lee MK, Shim HJ, Park SM (2004) *J Electrochem Soc* 151:C25
4. Mackinnon DJ, Brannen JM (1982) *J Appl Electrochem* 12:21
5. Robinson DJ, O'Keefe TJ (1976) *J Appl Electrochem* 6:1
6. Mackinnon DJ, Brannen JM, Morisson RM (1988) *J Appl Electrochem* 18:252
7. Karavasteva M, Karaivanov St (1993) *J Appl Electrochem* 23:763
8. Thomas BK, Fray DJ (1981) *J Appl Electrochem* 11:677
9. Chandran M (1999) *Bull Electrochem* 15:242
10. Oliveira EM, Finazzi GA, Carlos IA (2006) *Surf Coat Technol* 200:5978
11. Carlos IA, Malaquias MA, Oizumi MM, Matsuo TT (2001) *J P Sources* 92:56
12. Almeida MRH, Carlos IA, Barbosa LL, Carlos RM, Lima-Neto BS, Pallone EMJA (2002) *J Appl Electrochem* 32:763
13. Carlos IA, Siqueira JL, Finazzi GA, Almeida MRH (2003) *J P Sources* 117:179
14. Carlos IA, Almeida MRH (2004) *J Electroanal Chem* 562:153
15. Finazzi GA, Oliveira EM, Carlos IA (2004) *Surf Coat Technol* 187:377
16. Barbosa LL, Almeida MRH, Carlos RM, Yonashiro M, Oliveira GM, Carlos IA (2005) *Surf Coat Technol* 192:145
17. Pushpavanam M, Balakrishnan K (1996) *J Appl Electrochem* 26:283
18. Karwas C, Hepel T (1989) *J Electrochem Soc* 136:1672
19. Zech N, Landolt D (2000) *Electrochim Acta* 45:3461
20. Ji J, Cooper WC (1996) *Electrochim Acta* 41:1549
21. Wopschall RH, Shain I (1967) *Anal Chem* 39:1514
22. Hoare JP (1986) *J Electrochem Soc* 133:2491
23. Gilman S (1964) *J Electroanal Chem* 7:382
24. Barna GG, Frank SN, Teherani TH (1982) *J Electrochem Soc* 129:746
25. Lowenheim FA (1974) *Modern electroplating*, 2nd edn. Wiley, New York
26. Pereira MS, Barbosa LL, Souza CAC, Moraes ACM, Carlos IA (2006) *J Appl Electrochem* 36:727
27. Broggi RL, Oliveira GM, Barbosa LL, Pallone EMJA, Carlos IA (2006) *J Appl Electrochem* 36:403